REACTOR VESSEL OUTLET NOZZLE-TO-SHELL WELD FLAW INDICATION FRACTURE MECHANICS EVALUATION FOR POINT BEACH NUCLEAR PLANT, UNIT I

SwRI Project 17-7222-130

by

P. K. Nair

Prepared for:

Wisconsin Electric Power Company
231 W. Michigan, PO Box 2046
Milwaukee, Wisconsin 53201

March 27, 1984

8404030464 840330
PDR ADOCK 05000266
P PDR

TABLE OF CONTENTS

LIST OF TABLES

LIST OF FIGURES

LIST OF FIGURES

1.0 INTRODUCTION

During the spring of 1984's in-service examination of the Point Beach Unit reactor pressure vessel, several ultrasonic reflectors were detected in the outlet nozzle to shell welds. Two of the indications were found to be unacceptable by size limits of Table IWB-3512 of the ASME Section XI Code [1].

The purpose of this document is to provide a detailed fracture mechanics analysis of the marginally unacceptable indications by IWB-3512. Using the alternate acceptance criteria in IWB-3600, the long-term integrity of the vessel will be established.

2.0 TECHNICAL APPROACH

2.1 ASME BVP Code Section XI Appendix A

The detected flaw indications are analyzed using the linear elastic fracture mechanics method described in Appendix A of the ASME Section XI Code (1977). The analysis involves characterizing flaws in a regular elliptic shape and determining their stability using representative material properties and applicable loadings.

The Appendix A approach provides algorithms to compute stress intensity factors. The toughness properties are only available for lower-shelf and transition regions. Hence, upper-shelf toughnesses have to be estimated from surveillance and other weld data with similar chemistries. Irradiation degradation estimation procedures are also presented. Flaw acceptance criteria is based on the alternate criteria in IWB-3600 and expressed as follows:

$$K_{Ia}/K_{I} > \sqrt{10} \text{ for Levels I and II loadings}$$

and

$$K_{Ic}/K_{I} > \sqrt{2} \text{ for Levels III and IV loadings}$$

2.2 Flaw Characterization

Two major flaw indications are considered. These were individually found unacceptable by inspection criteria in Table IWB-3512 of Section XI. The location of these indications are, Flaw #2 at 28.5° vessel azimuth and Flaw #4 at 208.5° vessel azimuth. Associated with Flaw #2 is a satellite flaw indication with about 1% area of the Flaw #2 area. They are spaced in excess of the larger flaw diameter distance apart. The effect of the small flaw on Flaw #2 is considered negligible. Flaw #2 will be treated as an independent flaw for the analysis in this report. The #2 and #4 indications can be assumed to be radial-axial flaws in the vessel of 9.125 inches thick. This

assumption permits the flaw to be oriented perpendicular to the maximum principle stress direction.

The indications are completely circumscribed by elliptic area according to the IWA-3300 method.

3.0 FRACTURE MECHANICS INPUT DATA

To perform a fracture mechanics based analysis, several input data are required. These data include, in general, the material properties under irradiated conditions, loading/transient information and the stress intensity factor computation algorithms.

3.1 Material Data

Point Beach Unit I Reactor Vessel was manufactured by Babcock & Wilcox Co. in accordance with ASME Code Section III 1965 Edition and satisfying Code Case 1332-2.

The outlet nozzles (A-508 Class 2) were welded to the shell with Mu-Mo-Ni wire HT #8T1554B and Linde 80 flux lot #8479.

Weld Chemistry

C	Mn	P	S	Si	Cr	Ni	Mo	Cu
0.08	1.58	0.014	0.012	0.45	0.07	0.60	0.40	0.19

Charpy V-Notch at (10°F)

53 ft-lbs

42 ft-lbs

50 ft-lbs

Weld Tensile Properties

UTS	Yield Point	% Elongation	RA
88000 psi	73500 psi	25.0%	64.3%
86500 psi	71500 psi	26.5%	66.2%

The production welds were stress relieved at 1100°F-1150°F for approximately 11 hours.

RT_{NDT} and Upper-Shelf Charpy V-Notch

Preirradiated test data for both RT_{NDT} and Charpy V-notch (upper-shelf) is not available for the outlet nozzle weld. However, data from the

surveillance weld for Unit I is applicable. The vessel welds have comparable chemistry and heat treatment.

Weld Chemistry

C	Mn	P	S	Si	Cr	Ni	Mo	Cu
0.09	1.47	0.019	0.024	0.49	0.13	0.57	0.39	0.18-0.24

Stress Relief

at 1125°F, 11-1/4 hours, furnace cooled.

WCAP-8739 (3) presents the preirradiated and irradiated data for Unit I capsules. For the purposes of the fracture analysis, the surveillance weld data will be used. These include:

RT_{NDT} = 25°F preirradiated

C_V(upper-shelf) = 65 ft lbs preirradiated

Fluence Levels at Flaw Locations

Figure 3-1 shows the decay of fluence levels as a function of distance from the active core. The flaw indications are an average distance of 35 inches from the active case. From Figure 3-1, the multiplying factor is obtained as 1.5×10^{-3}.

Figure 3-2 presents the end of life radial fluence distribution for (E > 1.0 MeV) in the 6.5 inch thick beltline region. The nozzle region is 9.125 inches thick. Therefore, using Figure 3.2 to represent the outlet nozzle region would be conservative. Since one of the indication crack tips is located at about 0.55t, the end-of-life fluence level is taken to be 1.1×10^{19} (at the beltline) $\times 1.5 \times 10^{-3}$ (multiplying factor for nozzle). Therefore, the maximum fluence level at the flaw locations will be 1.65×10^{16} n/cm^2.

On the basis of 1.65×10^{16} n/cm^2(E 1.0 MeV) fluence and Cu = 0.20%, P = 0.0.019 there is no irradiation effect on both RT_{NDT} and C_V (upper-shelf)

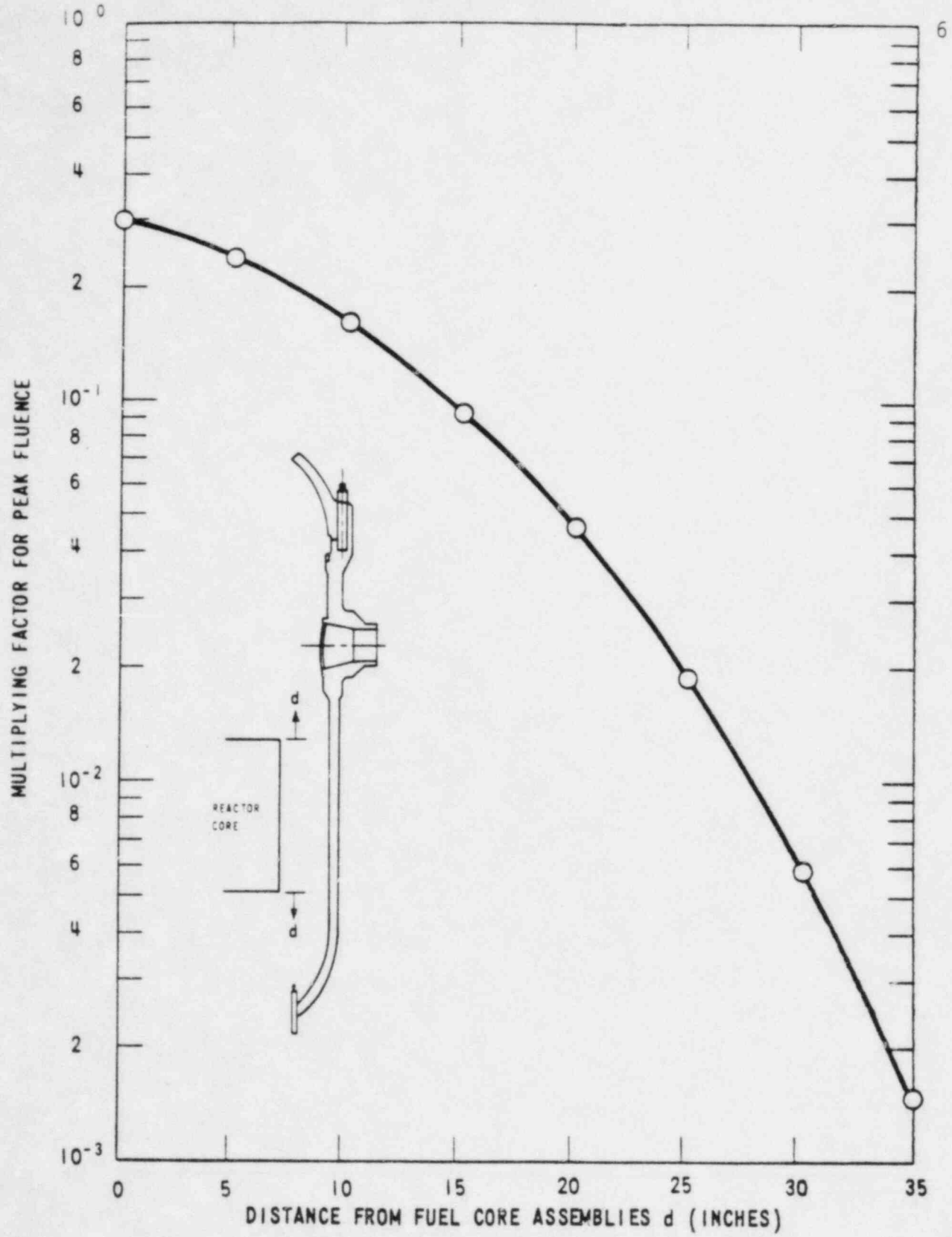

FIGURE 3-1. LONGITUDINAL DISTANCE VERSUS MULTIPLYING FACTOR FOR PEAK FLUENCE

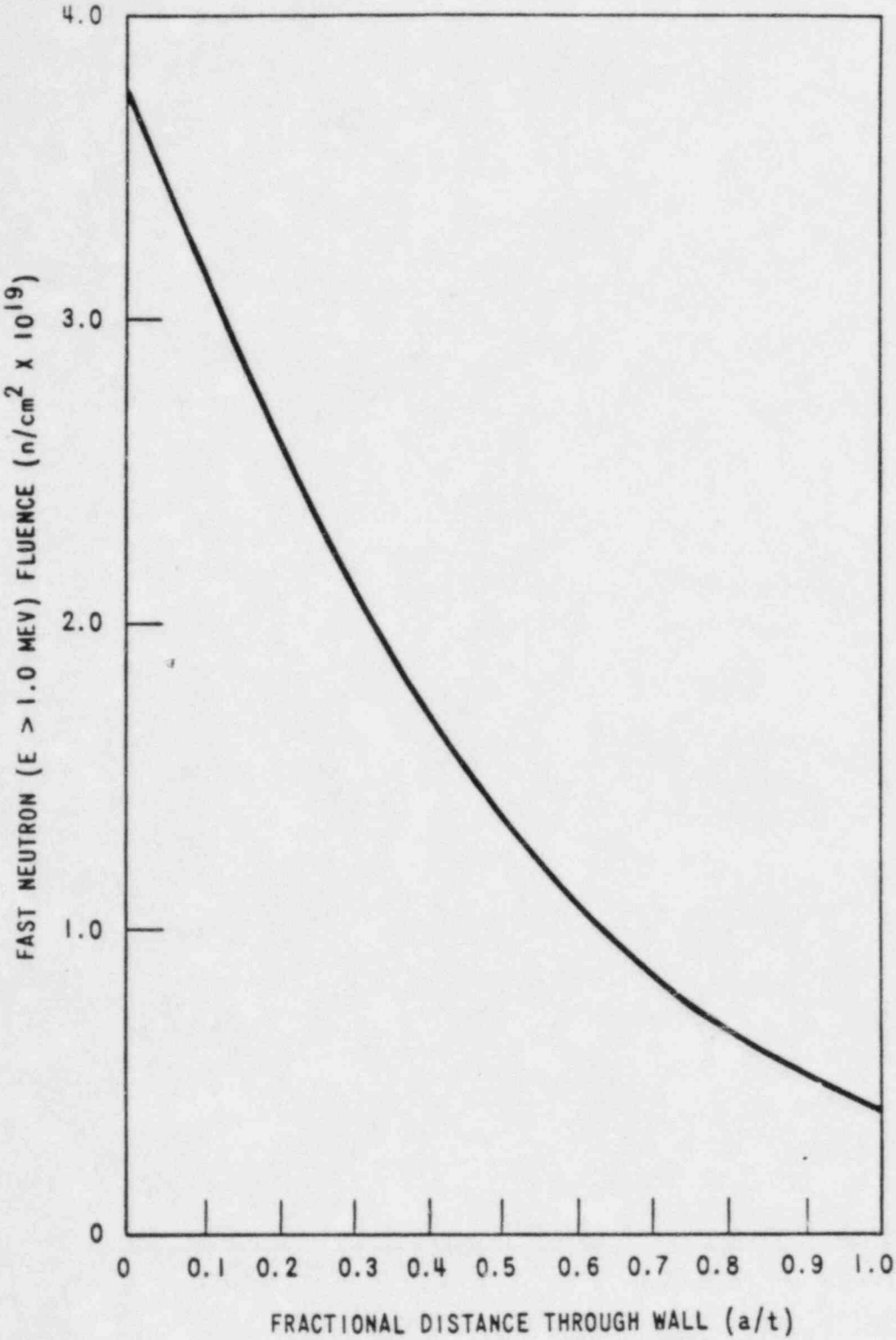

FIGURE 3-2. RADIAL FLUENCE DISTRIBUTION (MAXIMUM FLUENCE, 32 EFPY, 40 CALENDAR YEARS)

[Reference Reg. Guide 1.99, April 1977 Rev 1 (2)]. Therefore, the end of life values will be:

$RT_{NDT} = 25°F$

C_v(upper-shelf) = 65 ft lbs

Fracture Toughness Properties

For the lower-shelf and transition temperatures, Figure 3-3, i.e., Figure A 4200-1 of ASME Section XI Appendix A, will be used. This provides both the K_{1c}(static) and K_{1a}(arrest) toughness values.

At upper-shelf temperatures, both K_{1a} and K_{1c} are assumed to be equal. A very conserative estimate of toughness is obtained using the Barsom and Rolfe correlation from ASTM STP 466 (4).

i.e.,

$$\left(\frac{K_{Ic}}{\sigma_y}\right)^2 = \frac{5}{\sigma_y}\left[CVN - \frac{\sigma_y}{20}\right]$$

where σ_y is the yield stress (ksi)

CVN is the Charpy energy (ft lbs)

using σ_y = 72.500 ksi (average value)

and CVN = 65 ft lbs

$K_{Ic} = K_{Ia} = 149$ ksi $\sqrt{in}$

Fatigue Crack Growth

Data presented in ASME Section XI Appendix A Figure A-4300-1 (in air environment) will be used.

$$\frac{da}{dN} = 2.67 \times 10^{-11} \Delta K^{3.726}$$

where $\frac{da}{dN}$ is the crack growth per cycle

and ΔK is the stress intensity factor range.

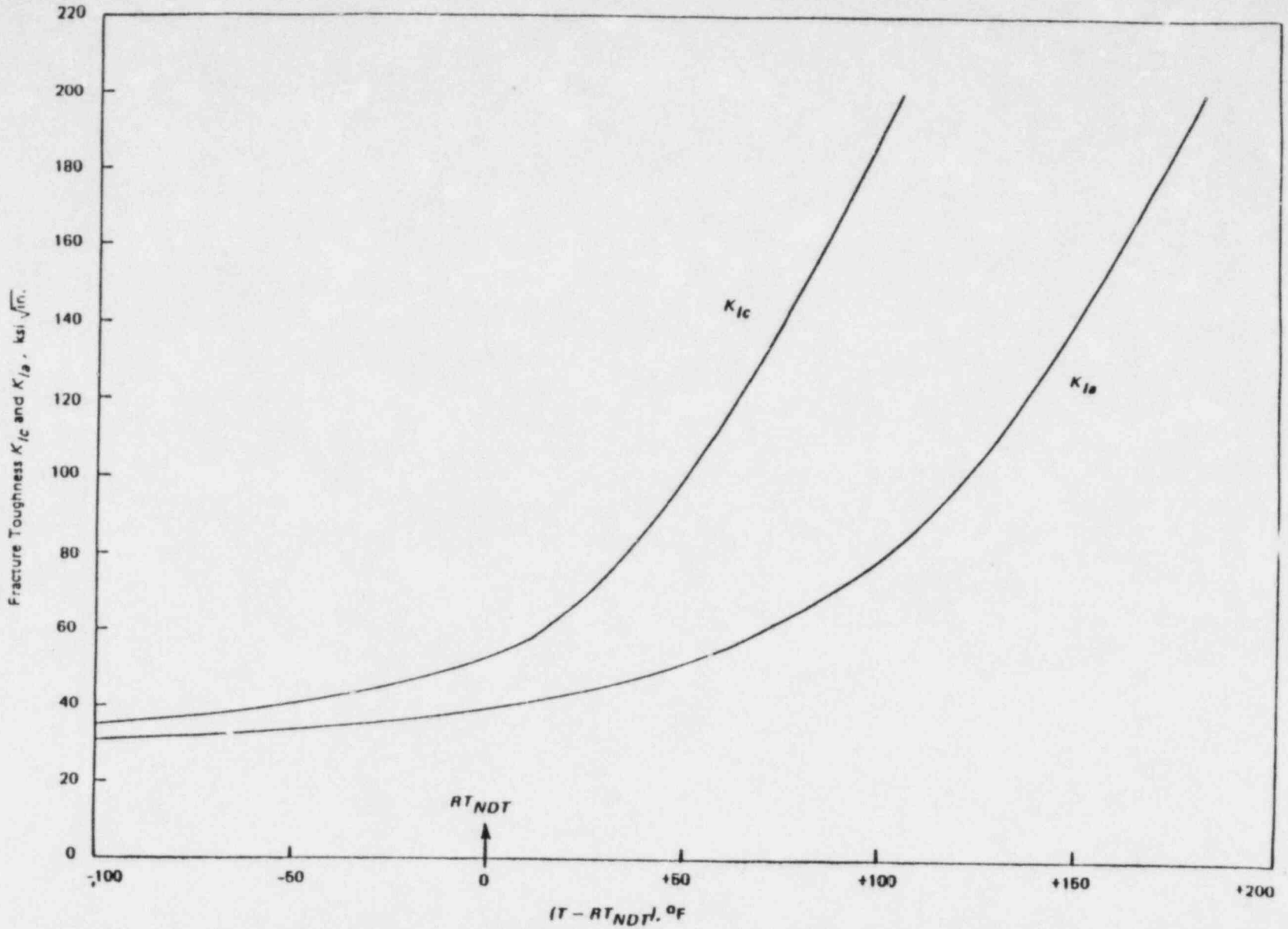

FIGURE 3-3. (Fig. A-4200-1) LOWER BOUND K_{ia} and K_{ic} TEST DATA FOR SA-533 GRADE B CLASS 1, SA-508 CLASS 2, AND SA-508 CLASS 3 STEELS

3.2 Loading and Stress Conditions

The various loading and stress conditons experienced under Levels I and II and postulated under Levels III and IV are discussed in this section.

3.2.1 Level I and II

Table 3.1 presents the Design Transients and Cycles for the vessel. (5)

Stress data for the outlet nozzle is presented in Table 3.2. Table 3.3 develops membrane and bending stress ranges with cycle information for the outlet nozzle.

3.2.2 Level III and IV

Three transients are considered in the evaluation. In selecting the transients, the relative magnitudes of the pressure and thermal stress components of the transients were studied. Thermal transients that decrease the coolant temperatures tend to create tensile stresses at the vessel ID. However, at the flaw locations of interest, compressive stresses are generated. These compressive stresses reduce the total tensile stress magnitude due to pressure at the flaw locations. In selecting the transients for evauation, the higher pressure transients have been evaluated.

For the purposes of the present analysis, the transient and thermal stresses temperatures data developed in WCAP-8742 (6) for the 6.5 inch thick vessel wall region will be conservatively assumed to be valid at the nozzle section. The temperature and stress distributions are developed for fractional distances of the vessel wall thickness. The transients analyzed below provide a bound on fracture conditions for all other postulated accidents.

TABLE 3.1 Design Transients and Cycles

TRANSIENTS	TIME	HOT LEG TEMP (°F) FOR OUTLET NOZZLE	PRESSURE (PSI)	DESIGN CYCLES	
				AT START UP	CURRENT TO END OF LIFE
Heatup Cooldown	4.5 hr 0 hr	547 547	2250 2250	200	150
Plant Loading Unloading	20 min 20 min	612 547	2250 2250	14500	10675
Small Step Load Increase	220 sec	610	2275	2000	1500
Small Step Load Decrease	35 sec	622	2320		
Large Step Load Decrease	2 min	588	2375	200	150
Loss of Load	10 sec	658	2775	80	60
Loss of Power	.75 hr	634	2550	40*	30
Loss of Flow	0 sec	614	2250	80	60
Reactor Trip From Full Power	0 sec	614	2250	400	300
Turbine Roll	0 min	614	2250	10	8
Steady State Fluctuations	+fluct.	620	2350	1.0×10^6	2.5×10^5
Cold Hydro	5 hr	100	3125	5	3
Hot Hydro	5 hr	400	2500	40	30

*ESTIMATED

TABLE 3.2 Stress Data for the Outlet Nozzle

Load Condition	Load Stage	Primary Stresses (ksi)				Secondary Stresses (ksi)				Total Stress (ksi)	
		σ_i	σ_o	σ_m	σ_b	σ_i	σ_o	σ_m	σ_b	σ_m	σ_b
Heatup Cooldown	4.5 HR 0 HR	33.53 33.53	23.43 23.43	28.48 28.48	5.05 5.05	-12.66 0.0	7.03 0.0	-2.82 0.0	-9.85 0.0	25.66 28.48	-4.8 5.05
Plant loading Unloading	20 MIN 20 MIN	33.53 33.53	23.43 23.43	28.48 28.48	5.05 5.05	-11.46 11.46	4.30 -4.30	-3.58 3.58	-7.88 7.88	24.90 32.06	-2.83 12.93
Small load step increase	220 SEC	33.88	23.78	28.83	5.05	0.87	-0.20	0.34	0.53	29.17	5.58
Small load step dec.	35 SEC	34.50	24.40	29.45	5.05	-1.86	0.13	-0.87	-0.99	28.58	4.06
Large load step dec.	2 MIN	35.27	25.17	30.22	5.05	-2.72	0.45	-1.14	-1.58	29.08	3.47
Loss of load	10 SEC	38.80	28.70	33.75	5.05	-10.39	0.42	-4.99	-5.40	28.76	-0.35
Loss of power	.75 HR	37.00	26.90	31.95	5.05	-2.58	1.26	-0.66	-1.92	31.29	3.13
Loss of flow	0 SEC	33.53	23.43	28.48	5.05	0.0	0.0	0.0	0.0	28.48	5.05
Reactor trip from full power	0 SEC	33.53	23.43	28.48	5.05	0.0	0.0	0.0	0.0	28.48	5.05
Turbine roll test	0 MIN	33.53	23.42	28.48	5.05	0.0	0.0	0.0	0.0	28.48	5.05
Steady state fluctuation	+ FLUCT.	34.92	24.82	29.87	5.05	-1.36	0.13	-0.62	-0.74	29.25	4.31
Cold hydro test	5 HR	45.65	35.55	40.60	5.05	0.0	0.0	0.0	0.0	40.60	5.05
Hot hydro test	5 HR	37.00	26.90	31.95	5.05	-7.55	4.72	-1.42	-6.13	30.53	-1.08

TABLE 3.3 Stress Ranges and Cycles Data

TRANSIENT NO.	LOAD CONDITION	CYCLES TO END OF LIFE	STRESS RANGES (KSI)	
			$\Delta\sigma_m$	$\Delta\sigma_b$
1	Heatup Cooldown	150	27.07	0.125
2	Plant loading Unloading	10,875	1.41	9.975
3	Small load Increase/Decrease	1,500	1.82	4.82
4	Large step Load Decrease	150	2.01	3.345
5	Loss of load	60	1.69	-0.475
6	Loss of power	30	4.22	3.005
7	Loss of flow	60	1.41	4.925
8	Reactor trip from full power	300	1.41	4.925
9	Turbine roll	8	1.41	4.925
10	Steady-state	2.5×10^5	2.18	4.180
11	Cold hydro	3	13.53	4.925
12	Hot hydro	30	3.44	-1.205

3.2.2.1 Loss of Coolant Accident

During LOCA, the reactor vessel rapidly depressurizes and safety injection commences. Initially, water at 90°F enters the vessel via the downcomer and 20 seconds later the injection pumps pump fluid from the BAST at a temperature of 155°F. After 53 seconds into the accident pump, suction transfers to the refueling water storage tank and the temperature is 33°F.

The injection flow from the safety injection pumps enters the RV downcomer through the inlet nozzle from the cold leg of the piping system. The outlet nozzles do not experience the initial thermal shock as much as the region near the inlet nozzles.

Overall, the pressure drops from 2250 psia to approximately 30 psia. In reference (6) WCAP-8742, the resulting LOCA temperature and stress profiles in the vessel wall were developed. These are reproduced here in Figures 3-4 and 3-5.

3.2.2.2 Steam Line Break Accident

During a large steam line break, the coolant temperature and pressure decreases rapidly. Safety injection is triggered when the coolant pressure falls below 1560 psia. The injection flow rates depend on the assumptions for reactor coolant system back pressure and for one or two loop cold leg flows. The details of the transients are described in WCAP-8742 (6).

For the purposes of the current evaluation, two cases of the large steam line break are considered. In the first case, off site power is assumed available throughout and the coolant flow is maintained. In the second case, a loss of off site power and the coolant system flow coastdown is assumed. Figure 3-6 shows the pressure variation and Figure 3-7

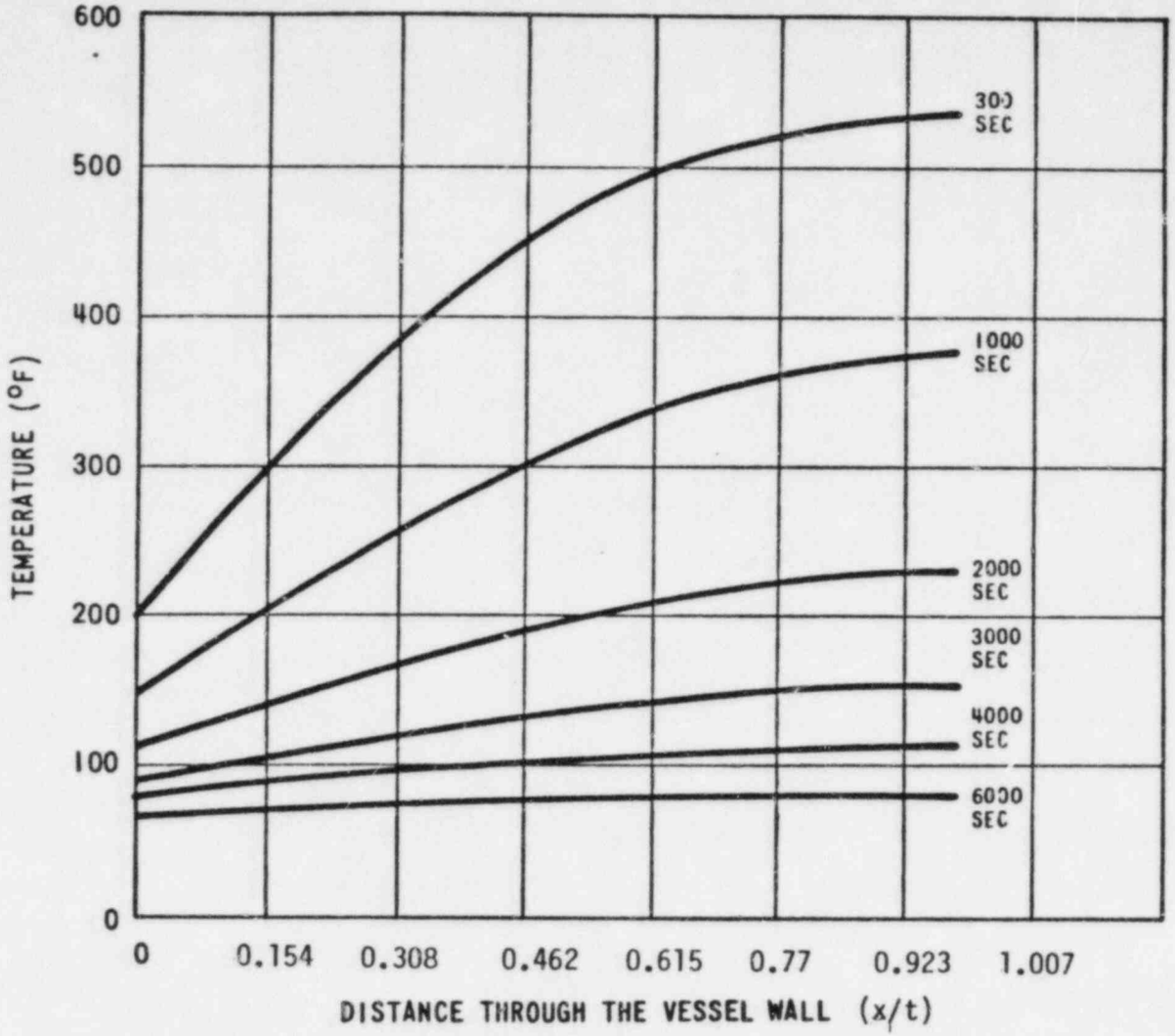

FIGURE 3-4. TEMPERATURE DISTRIBUTION THROUGH THE VESSEL WALL FOR A LARGE LOSS-OF-COOLANT ACCIDENT

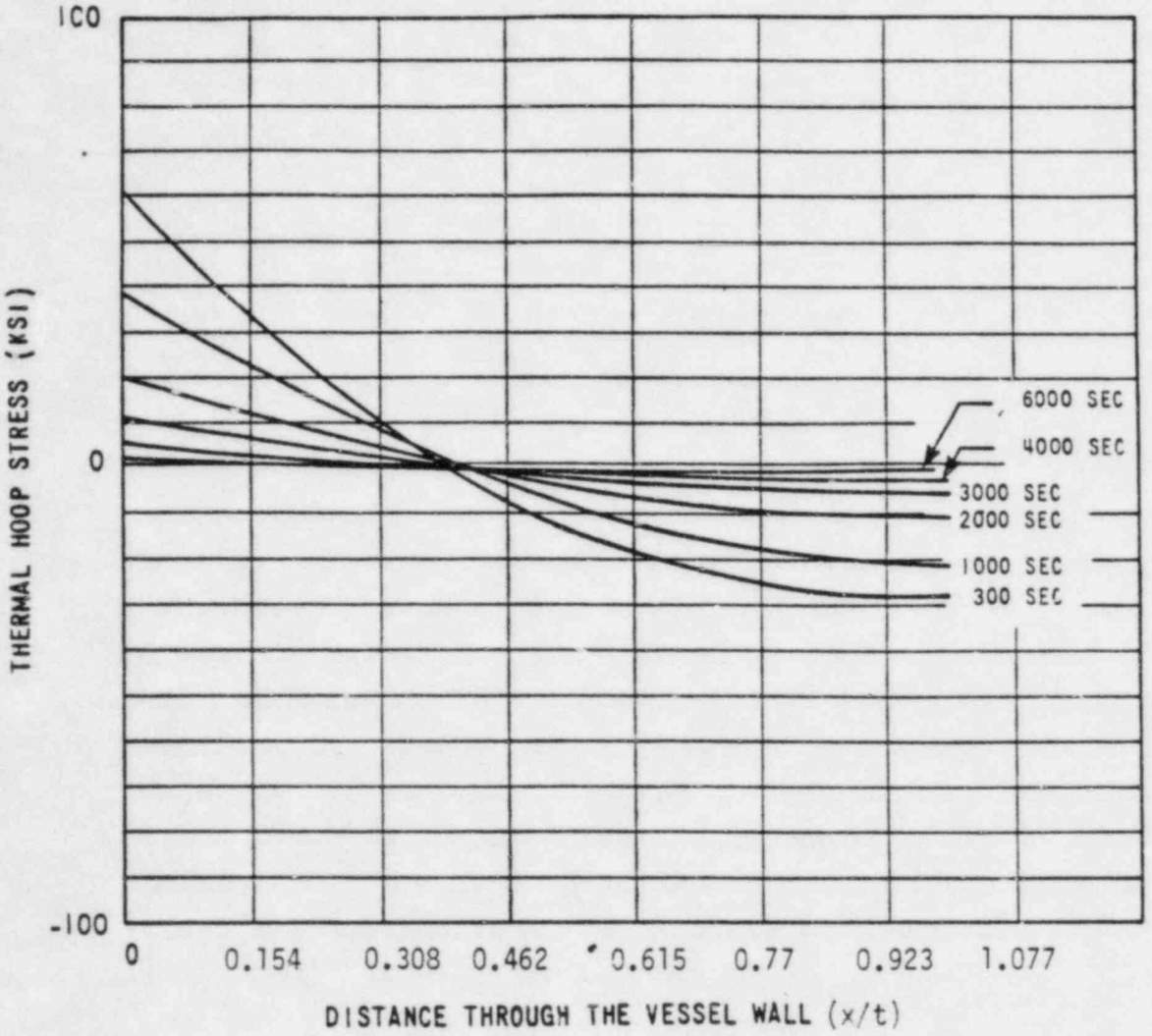

FIGURE 3-5. THERMAL HOOP STRESS THROUGH THE VESSEL WALL FOR A LARGE LOSS-OF-COOLANT ACCIDENT

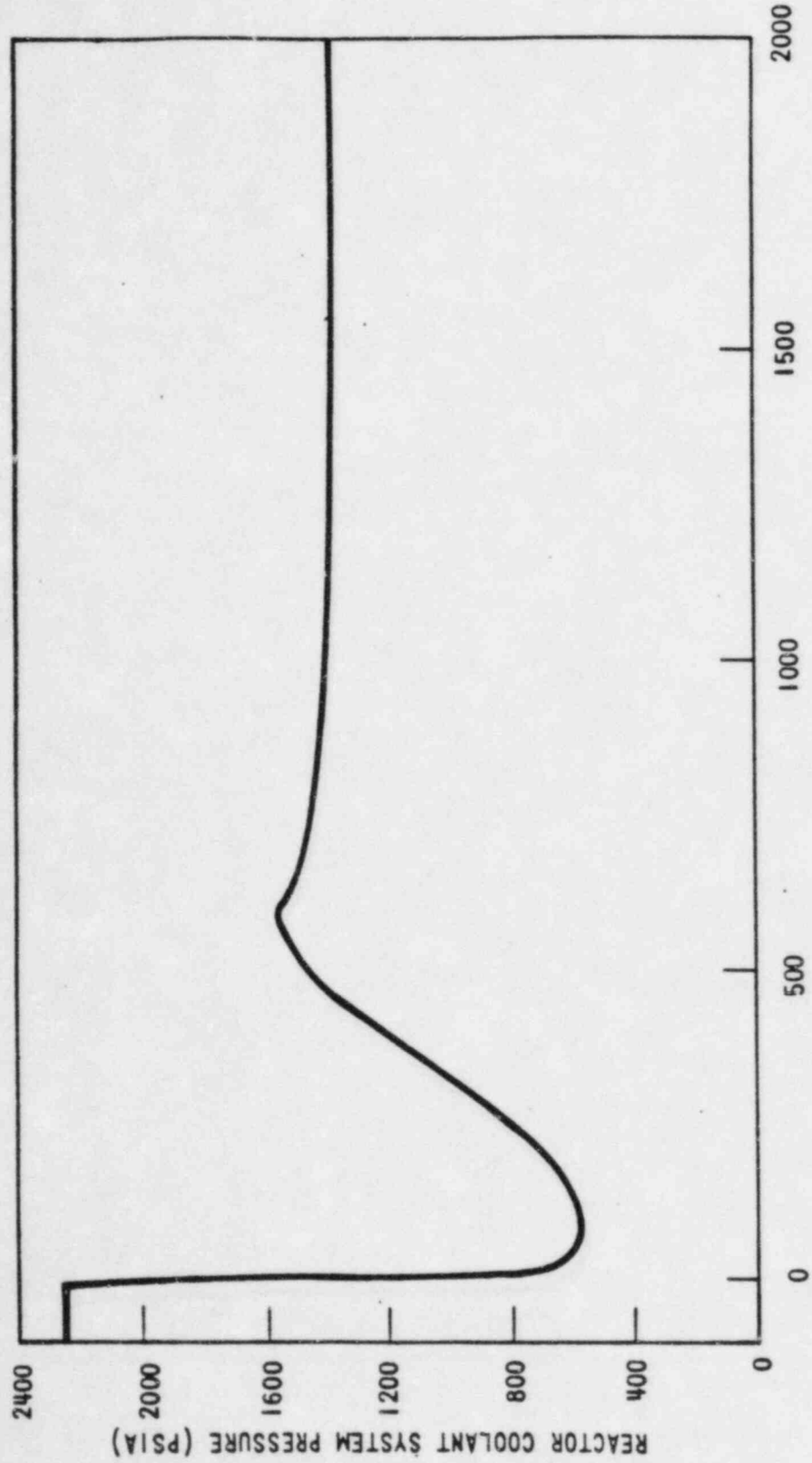

FIGURE 3-6. LARGE STEAM BREAK WITH REACTOR COOLANT PUMPS RUNNING; REACTOR COOLANT SYSTEM PRESSURE VERSUS TIME (SECONDS)

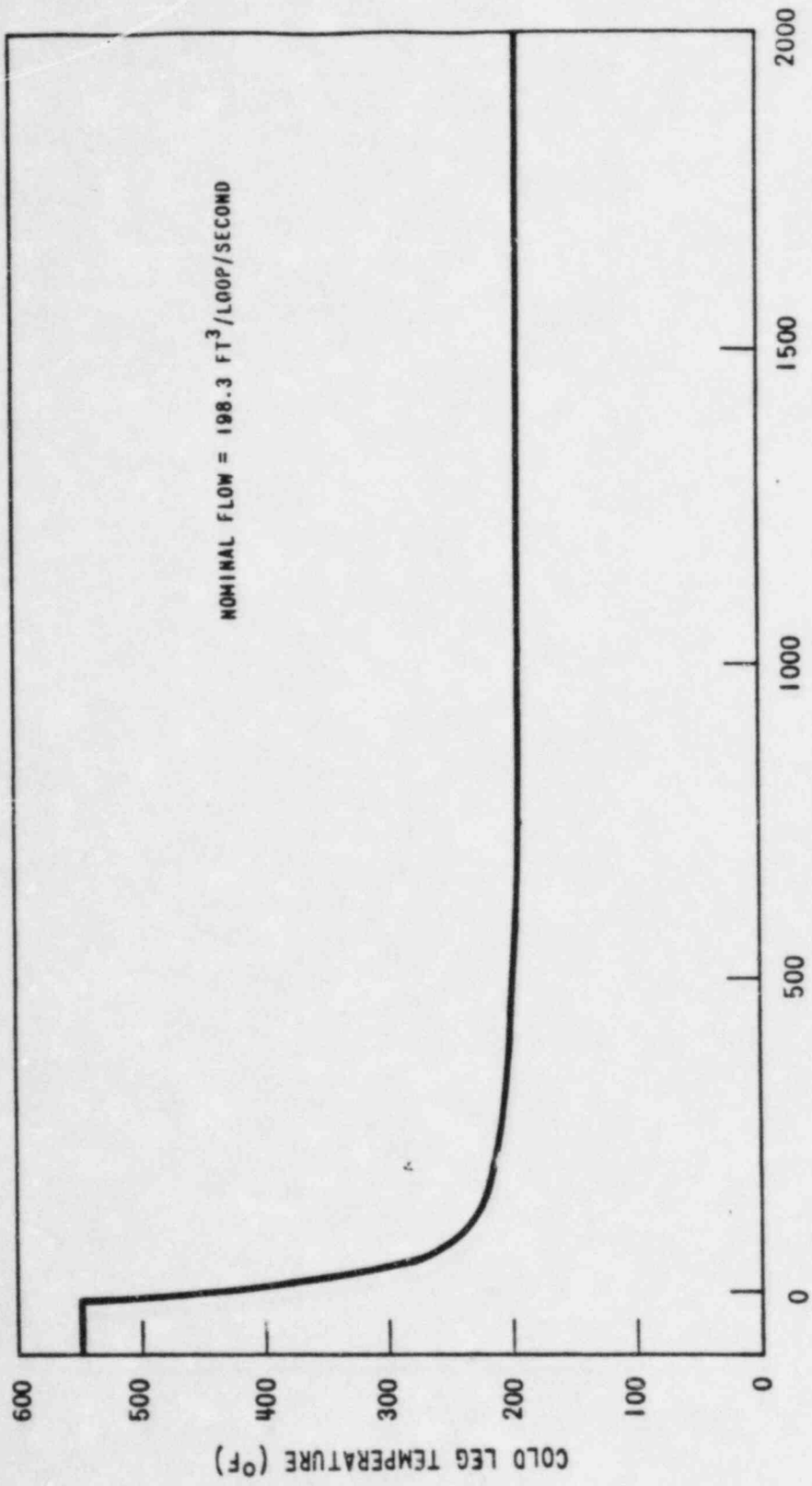

FIGURE 3-7. LARGE STEAM BREAK WITH REACTOR COOLANT PUMPS RUNNING; COLD LEG TEMPERATURE VERSUS TIME (SECONDS)

presents the cold leg temperature variation for the first case. The resulting vessel wall temperatures and the hoop stresses are presented in Figures 3-8 and 3-9, respectively.

For the second case, Figures 3-10 and 3-11 describe the pressure and temperature transients respectively. The vessel wall temperatures and loop stresses are shown in Figures 3-12 and 3-13 respectively. Reactor coolant system flow is rapidly reduced and the reactor trips at the low-flow signal.

3.2.2.3 Locked Rotor Accident

During this postulated accident, the instantaneous seizure of a reactor coolant pump rotor is assumed. The flow through the reactor coolant system is rapidly reduced and the reactor trips at the low-flow signal. Following the trip, heat stored in the fuel rods continues to heat up and expand the coolant. The transient is described in the Unit I FSAR and PSAR. The pressure transient is presented in Figure 3-14. The coolant temperature during the peak pressure of 2778 psia is assumed unchanged at the outlet nozzle and is at operating temperatures.

3.3 Stress Intensity Factors

The flaw characterized earlier will be analyzed using the ASME Section XI Appendix A approach. Stress intensity factors for any given flaw is calculated as (Article A-3000).

$$K_1 = (\sigma_m M_m + \sigma_b M_b)\sqrt{\frac{\pi a}{Q}} \qquad 3.1$$

where K_1 = stress intensity factor

σ_m, σ_b = membrane and bending stresses

M_m, M_b = membrane and bending correction factors

$2a$ = through wall crack penetration

Q = flaw shape parameter

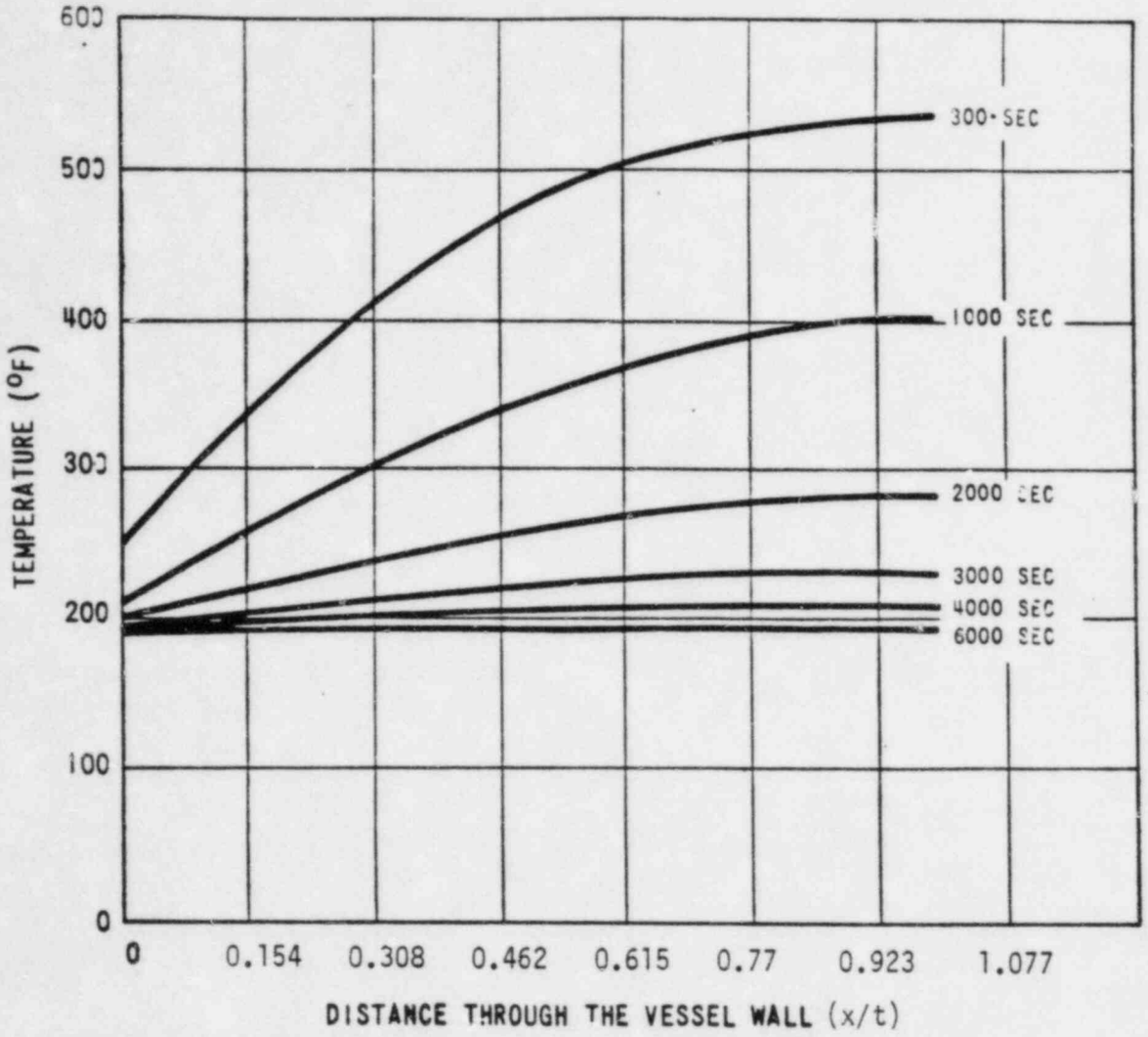

FIGURE 3-8. TEMPERATURE DISTRIBUTION THROUGH THE VESSEL WALL FOR A LARGE STEAM LINE BREAK WITH OFF-SITE POWER AVAILABLE

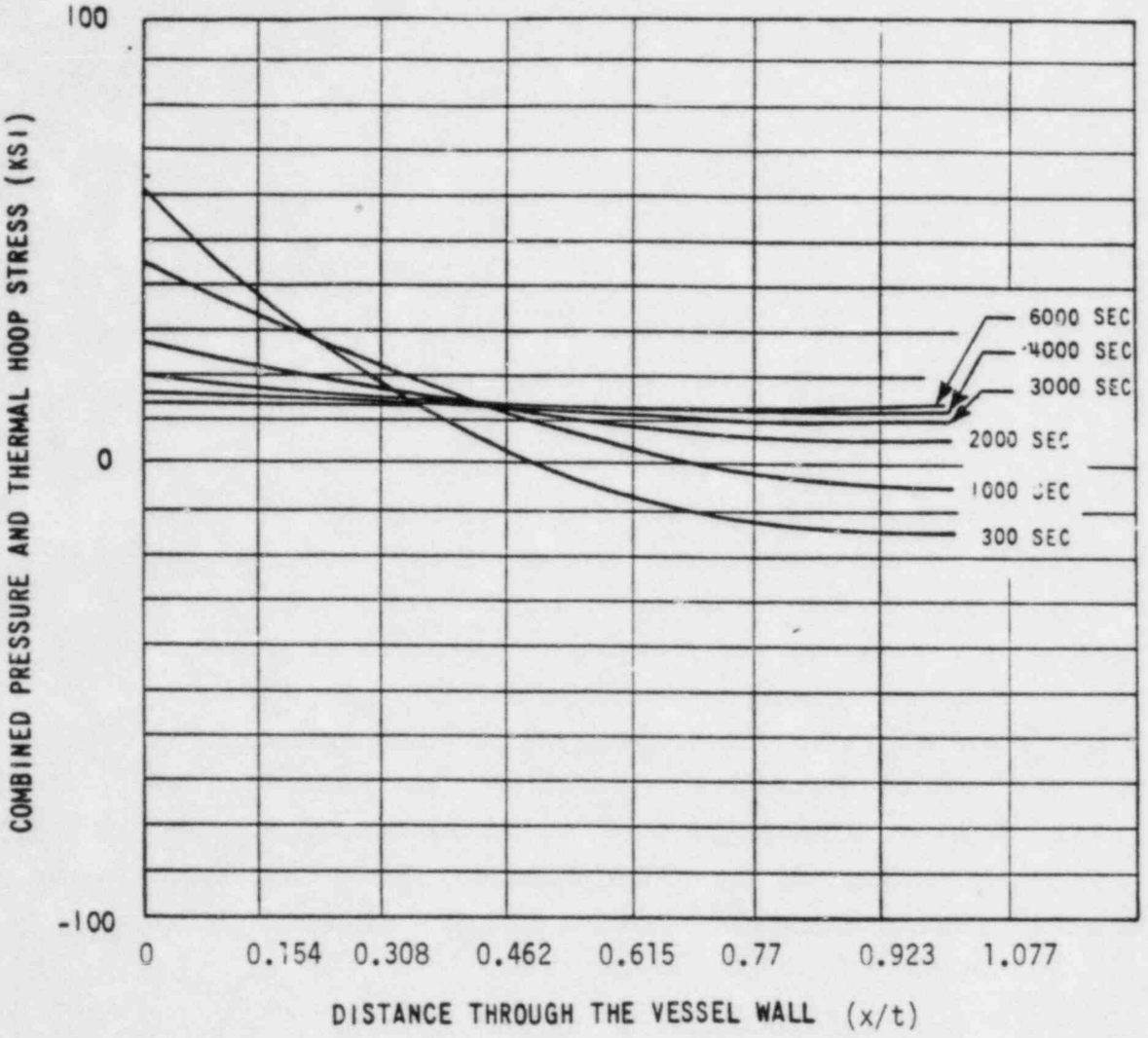

FIGURE 3-9. PRESSURE AND THERMAL HOOP STRESS DISTRIBUTION THROUGH THE VESSEL WALL FOR A LARGE STEAM LINE BREAK WITH OFF-SITE POWER AVAILABLE

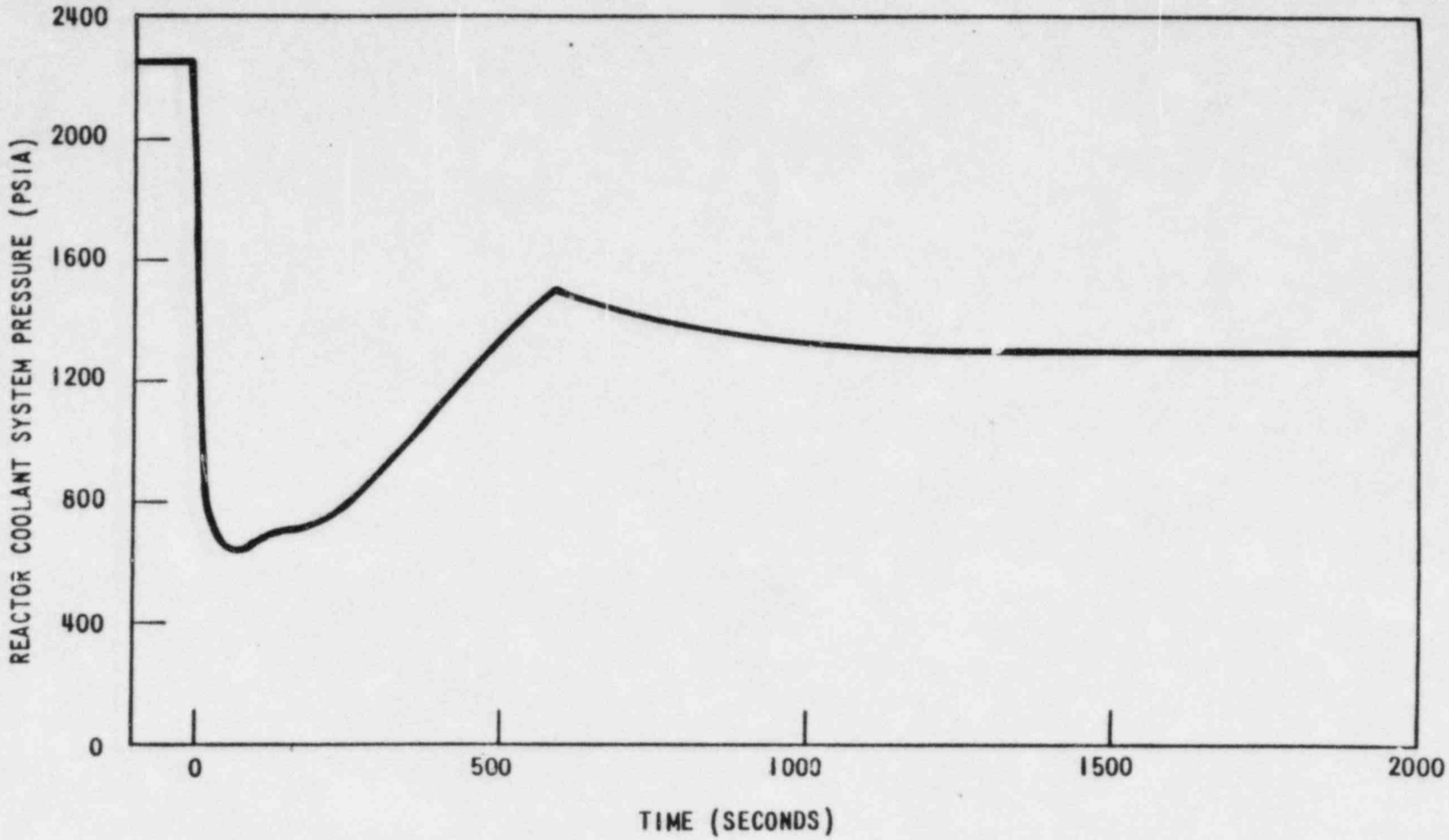

FIGURE 3-10. LARGE STEAM BREAK WITH REACTOR COOLANT PUMPS TRIPPED; REACTOR COOLANT SYSTEM PRESSURE VERSUS TIME (SECONDS)

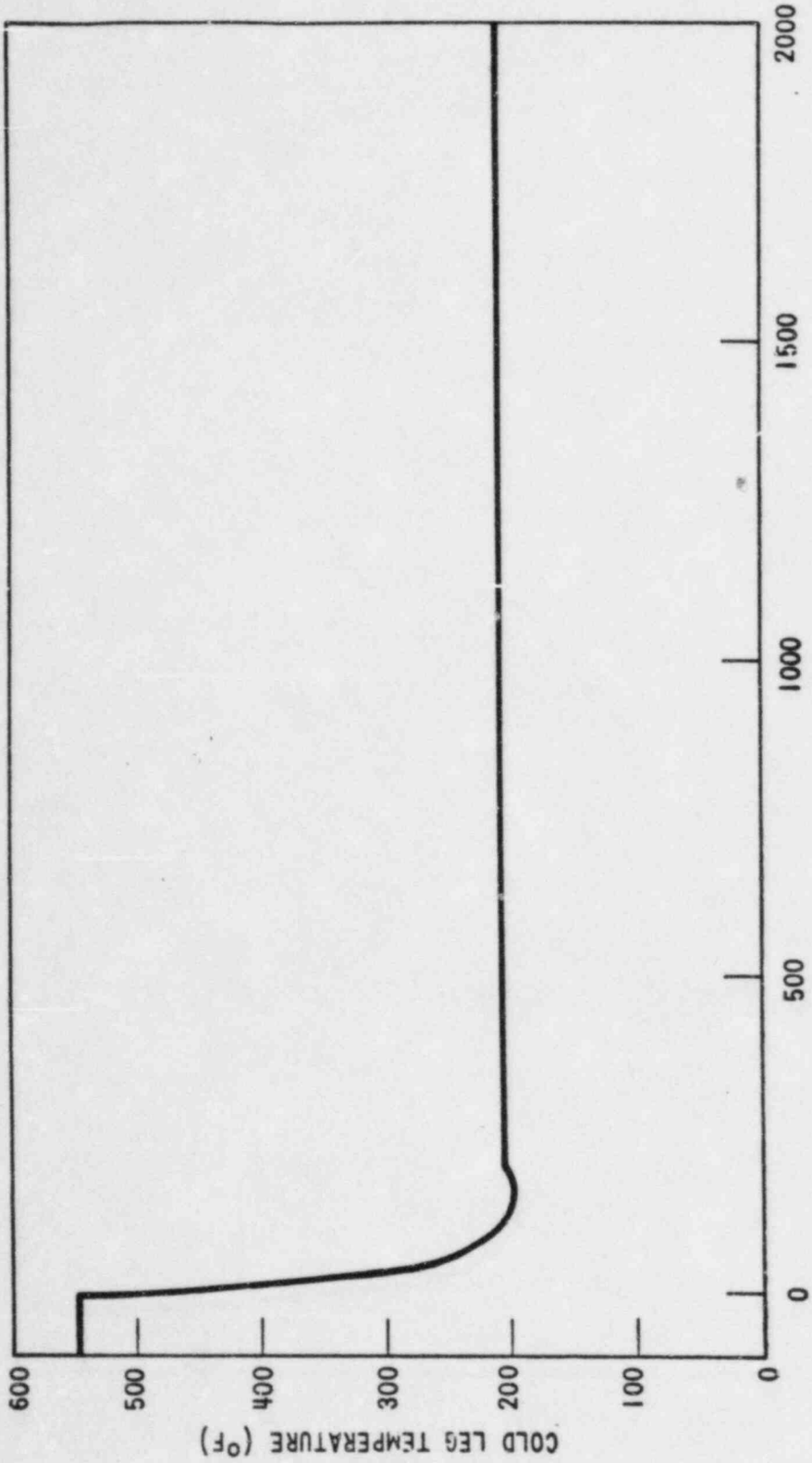

FIGURE 3-11. LARGE STEAM BREAK WITH REACTOR COOLANT PUMPS TRIPPED; COLD LEG TEMPERATURE VERSUS TIME (SECONDS)

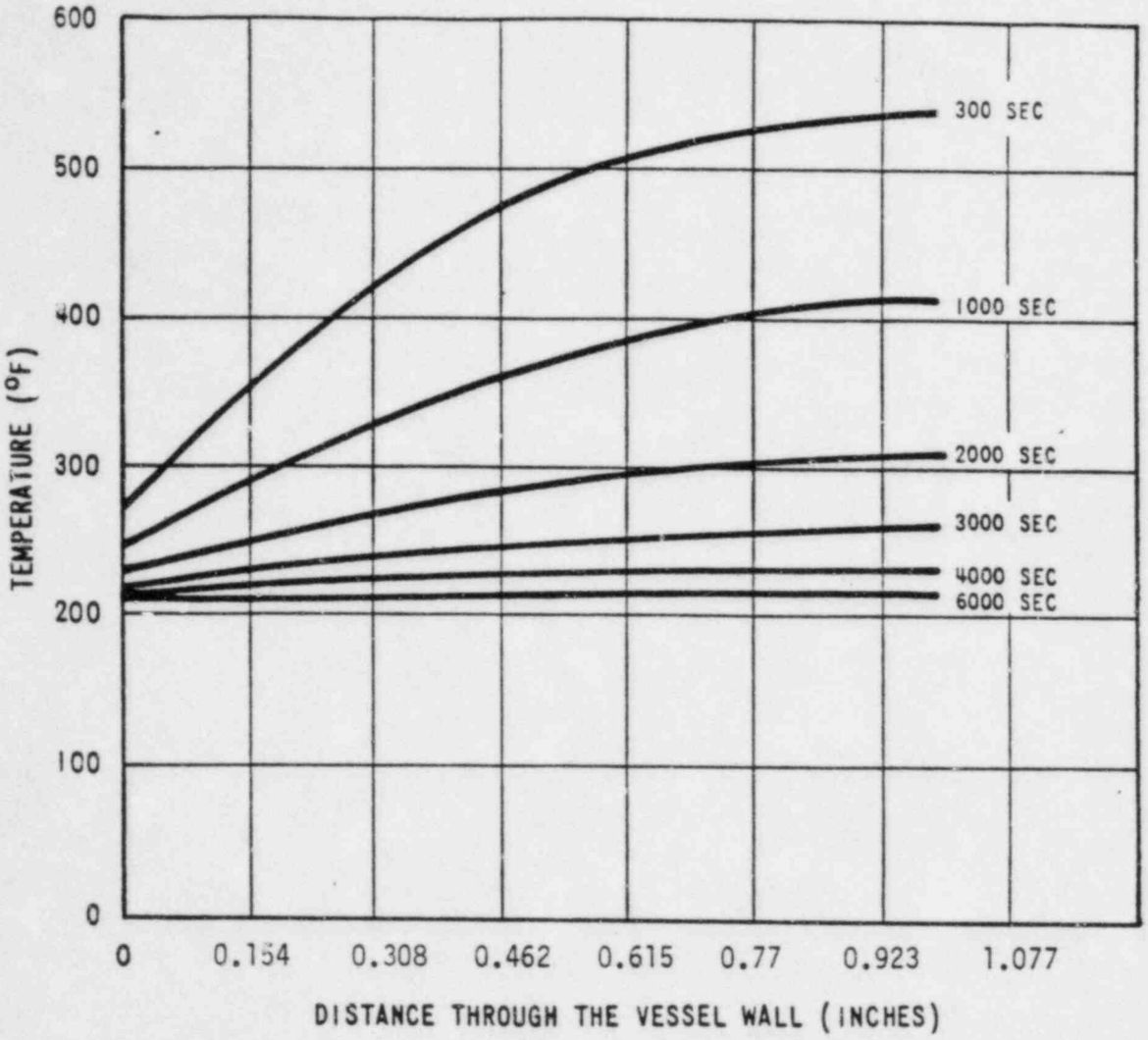

FIGURE 3-12. TEMPERATURE DISTRIBUTION THROUGH THE VESSEL WALL FOR A LARGE STEAM LINE BREAK WITHOUT OFF-SITE POWER

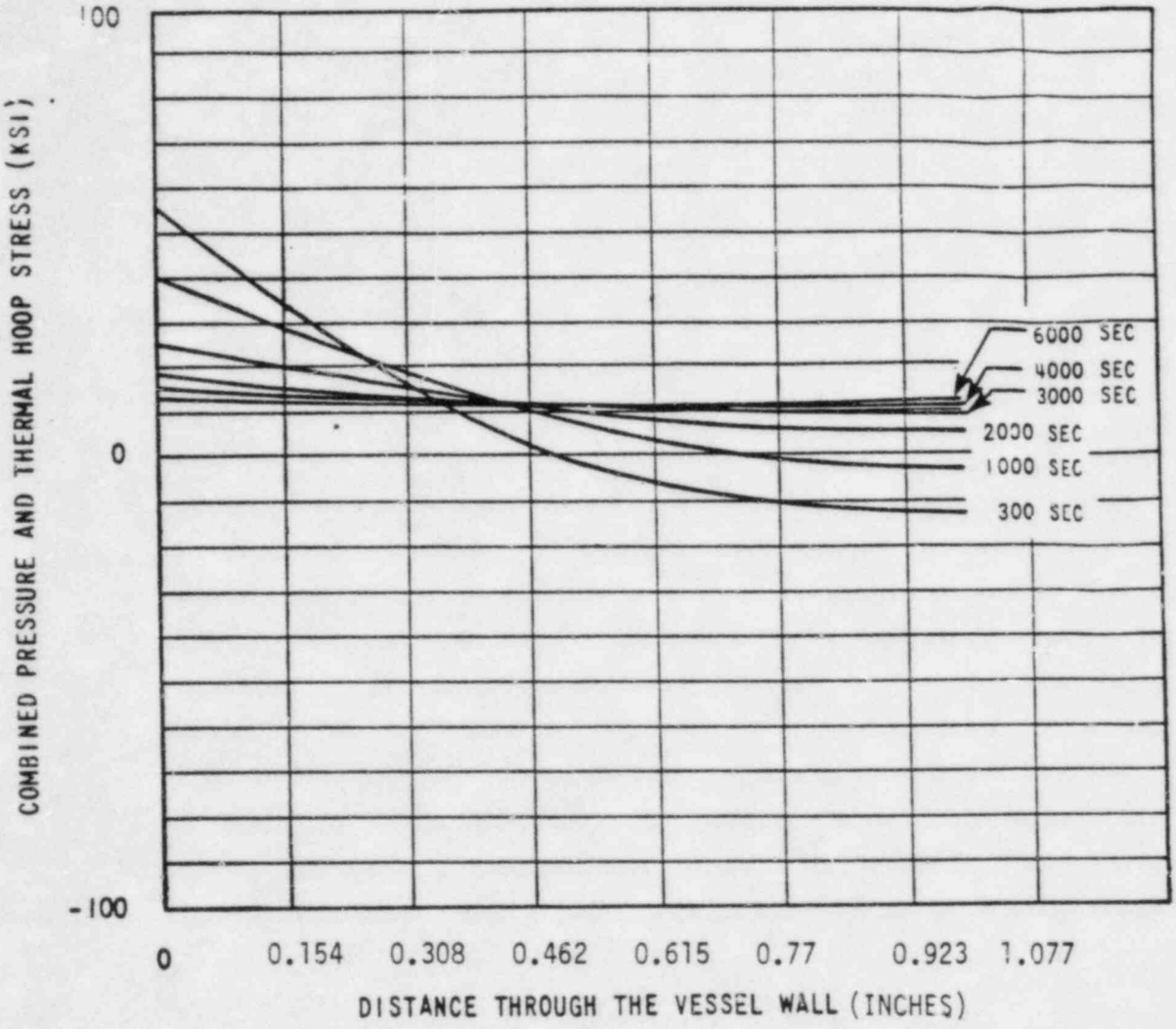

FIGURE 3-13. PRESSURE AND THERMAL HOOP STRESS DISTRIBUTION THROUGH THE VESSEL WALL FOR A LARGE STEAM LINE BREAK WITHOUT OFF-SITE POWER

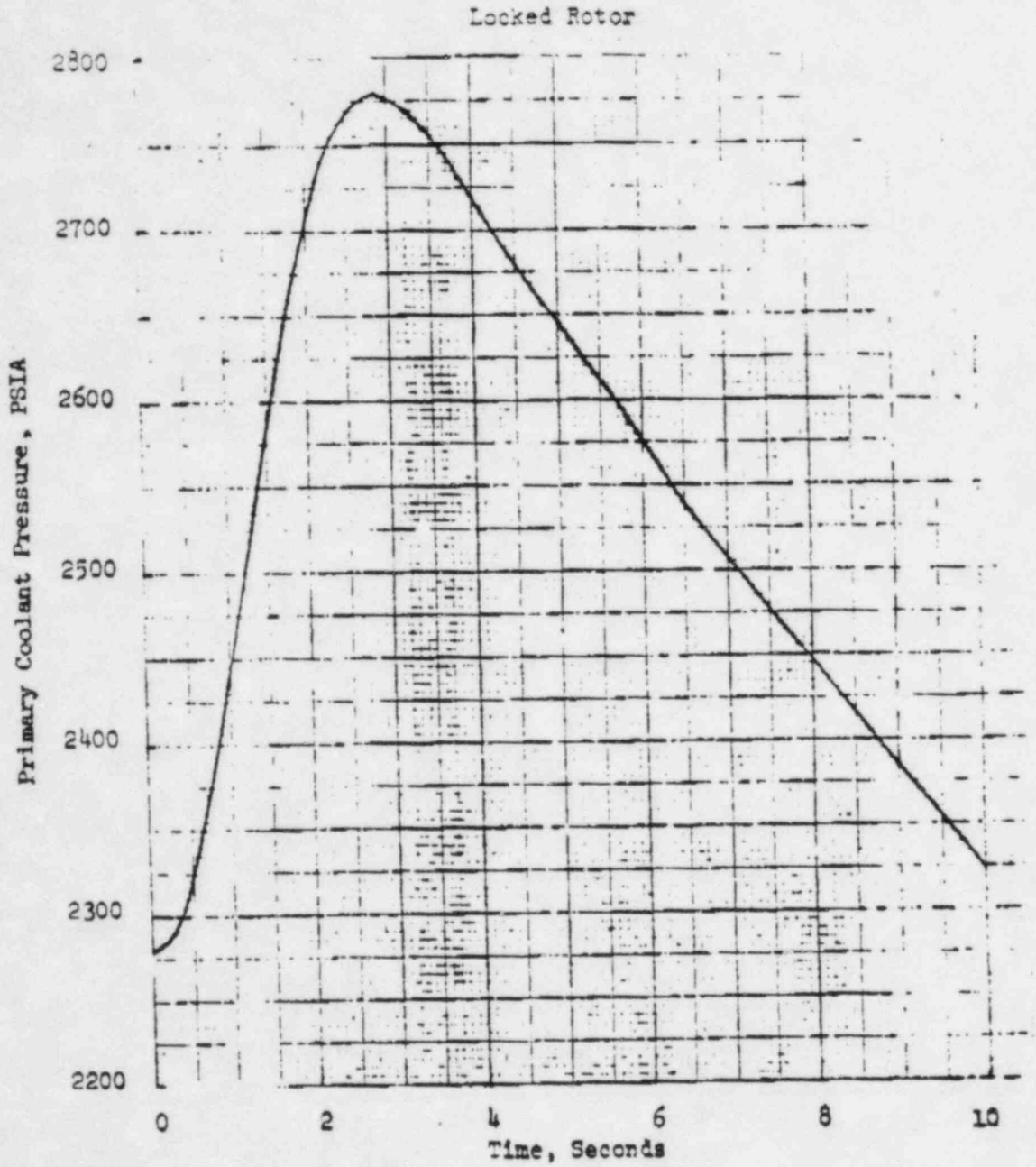

FIGURE 3-14. LOCKED ROTOR PRESSURE TRANSIENT

3.3.1 Flaw #2

The following are the flaw parameters:

flaw location = 3/4t from ID

t = 9.125 inches

2a = 1.24 inches

ℓ = flaw length = 1.935 inches

a/ℓ = 0.32

Q = 1.55 for $\frac{\sigma m + \sigma b}{\sigma ys} = 0.6$

e = flaw eccentricity = 0.25t

$\frac{2a}{t} = 0.14$

From Figures A-33003-2 and A-3300-4, the correction factors for locations pt_1, and pt_2 as shown in the sketch below are:

M_m = 1.03 for pt_1

= 1.02 for pt_2

M_b = 0.6 for pt_1

= 0.45 for pt_2

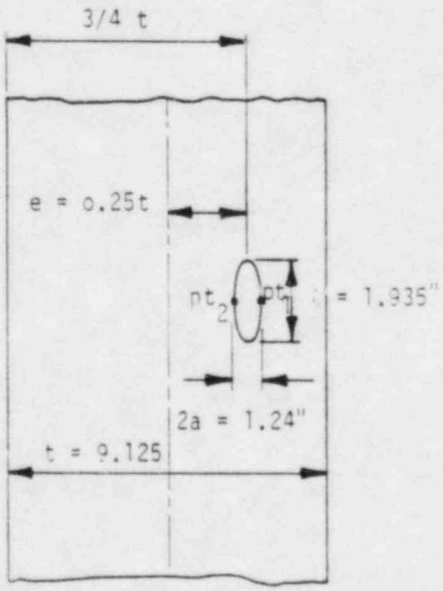

FIGURE 1. FLAW #2 PARAMETERS.

Equation 1 for pt_1 and pt_2 can be written as:

for pt_1 $K_1 = 1.424\ (1.03\ \sigma_m \pm 0.6\sigma_b)\ \sqrt{a}$ 3.2

for pt_2 $K_1 = 1.424\ (1.02\ \sigma_m \pm 0.45\sigma_b)\ \sqrt{a}$ 3.3

3.3.2 Flaw #4

The following are flaw parameters:

flaw location = 0.56t from ID and at 311° around nozzle

$t = 9.125$ inches

$2a = 1.14$ inches

$\ell = 1.29$ inches

$\frac{a}{\ell} = 0.44$

$Q = 2.1$ for $\frac{\sigma_m + \sigma_b}{\sigma_{ys}} = 0.6$

$e = 0.06t$

$\frac{2a}{t} = 0.125$

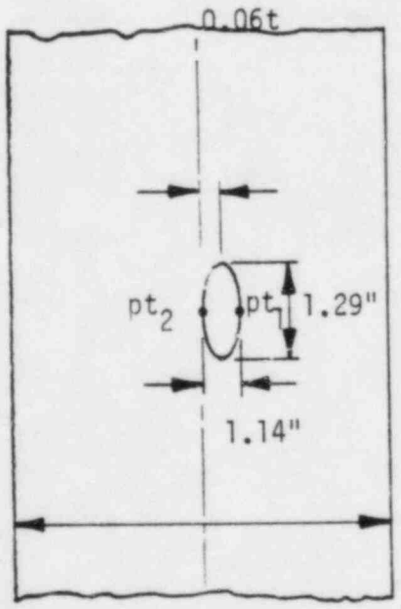

FIGURE 2. FLAW #4 PARAMETERS.

Correction factors for pt_1 and pt_2 in Figure 2 are:

$M_m = 1.02$ for pt_1

$= 1.02$ for pt_2

$M_b = 0.2$ for pt1

$= 0.05$ for pt_2

Stress intensity factors for pt_1 and pt_2 are:

for pt_1 $\quad K1 = 1.223\ (1.02\sigma_m \pm 0.2\sigma_b)\ \sqrt{a}$ 3.4

for pt_2 $\quad K1 = 1.223\ (1.02\sigma_m \pm 0.05\ \sigma_b)\ \sqrt{a}$ 3.5

4.0 FRACTURE INTEGRITY EVALUATION

4.1 Normal and Upset Conditions (Levels I and II)

Under Levels I and II loading cases, the detected indications are analyzed for fatigue crack growth to end of life conditions. The flaw stability for the final crack size is evaluated. The acceptance criteria to be used is:

$$\frac{K_{1a}}{K_1} = \sqrt{10}$$

4.1.1 Fatigue Crack Growth Analysis

Fatigue crack growth is represented by (ASME Section XI App. A Figure A-4300-1).

$$\frac{da}{dN} = 2.67 \times 10^{-11} \Delta K^{3.726} \qquad 4.1$$

$$\text{where } \Delta K = (M_m \Delta\sigma_m + M_b \Delta\sigma_b)\sqrt{\frac{\pi a}{Q}} \qquad 4.2$$

Substituting equation 4.2 in equation 4.1 and integrating the following expression is obtained

$$a_f = [a_i^{-0.863} - 0.863\ 2.67 \times 10^{-11} (M_m \Delta\sigma_m + M_b \Delta\sigma_b)^{3.726} \left(\frac{\pi}{Q}\right)^{1.863} \Delta N]^{\frac{-1}{0.863}} \qquad 4.3$$

where a_f = final crack depth

a_i = initial crack depth

ΔN = number of cycles

Fatigue Crack Growth for Flaw #2

Substituting the various flaw parameters for flaw #2, Equation 4.3 becomes:

for pt_1

$$a_f = [a_i^{-0.863} - 8.593 \times 10^{-11}(1.03\sigma_m \pm 0.6\sigma_b)^{3.726} \Delta N]^{-1.16} \qquad 4.4$$

for pt_2

$$a_f = [a_i^{-0.863} - 8.593 \times 10^{-11}(1.02\sigma_m \pm 0.45\sigma_b)^{3.726}\Delta N]^{-1.16} \quad 4.5$$

Table 4-1 presents the end of life crack growth resulting from the expected transients. It is seen that the present crack of depth $2 \times a_i = 2 \times 0.62 = 1.24$ inches will grow to a crack $2 \times a_f = 2 \times 0.625 = 1.25$ inches by end of life.

Fatigue Crack Growth for Flaw #4

The following equations represent crack growth for Flaw #4.

at pt_1

$$a_f = [a_i^{-0.863} - 4.88 \times 10^{-11}(1.02\sigma_m \pm 0.2\sigma_b)^{3.726}\Delta N]^{-1.16} \quad 4.6$$

at pt_2

$$a_f = [a_i^{-0.863} - 4.88 \times 10^{-11}(1.02\sigma_m \pm 0.05\sigma_b)^{3.726}\Delta N]^{-1.16} \quad 4.7$$

Table 4-2 presents the cumulative crack growth for crack #3 to end of life. The total growth is seen to be insignificant.

4.1.2 Flaw Integrity Assessment

For all operating and upset load conditions, the minimum temperatures at the flaw locations are considerably in excess of the material RT_{NDT}, again

$$\frac{K_{Ia}}{K_1} = \frac{149}{38.02} = 3.92 > \sqrt{10}$$

Therefore, the flaw is acceptable.

TABLE 4.1 Fatigue Crack Growth - Flaw No. 2

TRANSIENT NO.	NO. OF CYCLES	CRACK GROWTH AT Pt_1		CRACK GROWTH AT Pt_2	
		a_i inches	a_f inches	a_i inches	a_f inches
1	150	0.62	0.6211876651	0.62	0.62113
2	10,875	0.62119	0.621657	0.62113	0.62115
3	1,500	0.621657	0.621657	0.62115	0.62115
4	150	No growth		No growth	
5	60				
6	30				
7, 8, 9	368				
10	2.5×10^5	0.621657	0.624778	0.62115	0.622813
11	3	No growth		No growth	
12	30				

TABLE 4-2. Fatigue Crack Growth - Flaw No. 3

TRANSIENT NO.	NO. OF CYCLES	CRACK GROWTH AT Pt_1		CRACK GROWTH AT Pt_2	
		a_i inches	a_f inches	a_i inches	a_f inches
1	150	0.57	0.570354	0.57	0.570353
2	10,875	0.570354	0.570354		
3	1,500	No growth calculated		No growth calculated	
4	150				
5	60				
6	30				
7, 8, 9	368				
10	2.5×10^5				
11	3				
12	30				

4.2 Emergency and Accident Conditions (Levels III and IV)

The acceptance criteria for flaw to withstand crack initiation under Level III or IV loading is given by

$$\frac{K_{Ic}}{K_1} > \sqrt{2}$$

Loss of Coolant Accident

From Figure 3-4 it can be seen that the temperatures during the 6000 sec transient duration are in excess of the end of life RT_{NDT} = 25°F for the flaw locations. Therefore, upper-shelf K_{1c} = 149 ksi $\sqrt{in.}$ will be assumed.

From Figure 3-5 the loop stresses are at all times dominated by bending stresses. Since the system is depressurized, there is no contribution due to pressure. The bending stresses at the flaw locations are compressive in nature. Hence, the stress intensity factor will be considered to be $K_1 = 0$

$K_1 = 0$ ksi $\sqrt{in.}$

Hence, crack initiation condition of

$$K_{1c}/K_1 > \sqrt{2} \text{ is satisfied.}$$

Large Steam Line Break

Case 1: With offsite power

The coolant temperature during the transient remains at about 200°F (see Figure 3-7 and 3-8). Therefore, here again upper-shelf material properties are assumed at the flaw locations and will be considered to be at upper-shelf conditions. In Section 2, the minimum end of life toughness was shown to be

$$K_{1c} = K_{1a} = 149 \text{ ksi } \sqrt{in.}$$

Flaw #2

End of life flaw dimension was calculated to be a_f = 0.625 inches. The flaw parameters are

$a/\ell = 0.32$

$2a_f = 1.25$ inches

The maximum stresses are obtained for the cold hydro transient (Refer Table 3-2).

$\sigma_m = 40.6$ ksi and $\sigma_b = 5.05$ ksi

The maximum stress intensity factor is obtained as

$K_1 = 43.5$ ksi $\sqrt{in.}$

The acceptance criteria

$$K_{Ia/K_1} = \frac{149}{43.5} = 3.45 > \sqrt{10}$$

is satisifed and hence, flaw is acceptable.

Flaw #4

End of life flaw dimensions

$a_f = 0.5704$ inches

Flaw parameters

$a/\ell = 0.44$

$2a_f = 1.141$ inches

For the cold hydro transient, maximum

$K_1 = 38.02$ ksi $\sqrt{in.}$

Figure 3-9 presents the combined pressure and thermal hoop stresses. The large bending component of the stress provides compressive stresses and hence, $K_1 = 0$ can be assumed.

Case 2: Without offsite power

Here also the temperatures are in excess of the material RT_{NDT} (Refer Figures 3-11 and 3-12).

The stresses shown in Figures 3-13 indicates the same behavior as Case 1 and $K_1 = 0$.

Locked Rotor Pressure Transient (Loss of Load)

Conditions: Metal temperatures in excess of 550° F

Max. Pressure = 2778 psia (Ref Figure 3-14)

Stress intensity computation:

σ_m = 33.75 ksi σ_b = 5.05 ksi

K_1 = (for Flaw #2) = 36.2 ksi $\sqrt{in.}$

Acceptance criteria:

$$K_{1c/K_1} = \frac{149}{36.2} = 4.1 > \sqrt{2}$$

5.0 CONCLUSIONS

The detected flaw indication #2 and #4 were analyzed using a linear elastic fracture mechanics approach. The approach conforms with the ASME Section XI requirements.

The analysis demonstrates that the flaws are stable under all postulated loading conditions. The margins of safety specified in ASME Section XI are adequately met. It is recommended that no repair is necessary for the detected flaw indications. The indications locations should be reinspected and monitored at the next scheduled nozzle weld inspection.

REFERENCES

1. ASME Boiler and Pressure Vessel Code, Section XI, 1977 Edition.

2. USNRC Reg. Guide 1-99 - "Effects of Residual Elements on Predicted Radiation Damage to Reactor Vessel Materials", Rev. 1, April 1977.

3. S. E. Yanichko and S. L. Anderson "Analysis of Capsule S from the Wisconsin Electric Power Company and Wisconsin Michigan Power Company Point Beach Nuclear Plant Unit No. 1 Reactor Vessel Radiation Surveillance Program," WCAP-8739, November 1976.

4. J. M. Barsom and S. T. Rolfe "Correlations Between K_{Ic} and Charpy V-Notch Test Results in the Transition-Temperature Range," Impact Testing of Metals, ASTM STP 466, June 1969, pp 281-302.

5. P. J. Fields, "ASME III, Appendix G Analysis of the Wisconsin Electric Power Company and Wisconsin Michigan Power Company Point Beach Nuclear Plant Unit No. 1 Reactor Vessel", WCAP-8741, September 1976.

6. T. A. Meyer, J. M. Kramps, S. Palusany, J. H. Phillips, P. J. Morris and R. W. Fleming "Fracture Mechanics Evaluation of the Wisconsin Electric Power Company and the Wisconsin Michigan Power Company Point Beach Nuclear Plant Unit No. 1 Reactor Vessel," WCAP 8742, February 1977.